ELSEVIER

Biophysical Chemistry 120 (2006) 87 – 95

Biophysical Chemistry

http://www.elsevier.com/locate/biophyschem

Inhibition of DNA hybridization by small metal nanoparticles

J. Yang [a,1], Jim Yang Lee [a,b,*], Heng-Phon Too [b,c], Gan-Moog Chow [b,d]

[a] *Department of Chemical and Biomolecular Engineering, National University of Singapore, 10 Kent Ridge Crescent, Singapore 119260, Singapore*
[b] *Singapore-MIT Alliance, 4 Engineering Drive 3, National University of Singapore, Singapore 117576, Singapore*
[c] *Department of Biochemistry, National University of Singapore, 10 Kent Ridge Crescent, Singapore 119260, Singapore*
[d] *Department of Materials Science and Engineering, National University of Singapore, 10 Kent Ridge Crescent, Singapore 119260, Singapore*

Received 1 September 2005; received in revised form 20 October 2005; accepted 21 October 2005
Available online 21 November 2005

Abstract

The inhibition of DNA hybridization by small metal nanoparticles has been examined in detail. DNA melting point analysis showed that the oligonucleotides adsorb strongly and nonspecifically on small metal nanoparticles, inhibiting the hybridization of complementary DNA sequences in common buffered solutions. The nonspecific interaction is even strong enough to disrupt pre-existing hydrogen bonds in short double-stranded DNA. The nonspecific interaction could be weakened by increasing the particle size. As an example, a core-shell assisted method was used to successfully assemble Pt nanoparticles by DNA hybridization that could not be done otherwise.

Keywords: Oligonucleotide; Nanoparticle; Non-specific interaction; Assembly; DNA hybridization

1. Introduction

After close to a decade of intense effort, DNA directed assembly of metal nanoparticles, Au nanoparticles in particular, has become a proven technique for DNA diagnostics, and for generating interesting one-, two- or three-dimensional nanostructured materials [1–23]. Mirkin's group, in particular, has developed several protocols to assemble Au nanoparticles based on the molecular recognition property of complementary DNA strands [4,8,16,18,23]. In their implementation, Au nanoparticles are first functionalized by oligonucleotides terminated with alkanethiol groups at the 3′ or 5′ end. Two non-complementary nucleotide sequences are used to functionalize two different batches of gold nanoparticles. Particle linking between the groups is initiated by adding a DNA linker with sticky ends complementary to the oligonucleotides adsorbed on the Au particles. A macroscopic network of particles held together by duplex DNA interconnects is formed as a result. Aggregated 13 [4,16,18], 31 and 50 nm Au nanoparticles [23] and binary nanoparticle networks containing 8 and 31 nm Au nanoparticles [8], have been successfully assimilated this way. However, difficulties arose when we tried to assemble smaller Au nanoparticles (5 nm) using the same methodology. No hybridization was detected when a matching DNA linker was added to the thiol-modified oligonucleotide-capped 5 nm Au particles. Further investigations revealed that pristine single stranded DNA (ssDNA, without any modification at the 3′ or 5′ end) is a good stabilizer for small Au nanoparticles in aqueous solution. As the gold nanoparticles are negatively charged, ssDNA could not easily approach the particle surface because of electrostatic repulsion unless there is strong ligation between the nucleotide backbone and the surface metal atoms. However, the stability of the ssDNA-Au bioconjugates does not depend strongly on the nucleotide sequence in the ssDNA. The interaction is therefore non-specific. The oligonucleotides in this case are recumbent on the nanoparticle surface and are therefore not optimally aligned for hybridization.

In this work, the nonspecific interaction between oligonucleotides and small metal nanoparticles is examined in detail by analyzing the solution stabilization of small Au nanoparticles capped by oligonucleotides and by the inhibition of DNA hybridization (according to DNA melting point measurements) in the presence of 5 nm Au nanoparticles. The inhibition of

* Corresponding author. Department of Chemical and Biomolecular Engineering, National University of Singapore, 10 Kent Ridge Crescent, Singapore 119260, Singapore. Tel.: +65 6874 2899; fax: +65 6779 1936.
E-mail address: cheleejy@nus.edu.sg (J.Y. Lee).
[1] Tel.: +65 6874 2899; fax: +65 6779 1936.

0301-4622/$ - see front matter © 2005 Elsevier B.V. All rights reserved.
doi:10.1016/j.bpc.2005.10.011

DNA hybridization appears to be a characteristic of small noble metal nanopartcles as it also occurs for Pt. The assembly of small metal nanoparticles by DNA hybridization therefore requires a prudent management of the nonspecific interaction. Herein we demonstrate a core-shell assisted growth method to artificially enlarge the Pt nanoparticles to reduce the nonspecific binding of oligonucleotides on the Pt surface, so as to enable particle assembly by DNA hybridization in subsequent steps.

2. Materials and methods

2.1. Materials and instrumentation

$HAuCl_4{\cdot}3H_2O$, $AgNO_3$, K_2PtCl_4 were purchased from Aldrich (Milwaukee, WI, USA). Sodium borohydride, $NaBH_4$ (98%), and sodium citrate dihydrate, $C_6H_5Na_3O_7{\cdot}2H_2O$ (98%), were supplied by Ajax (Alburn, Australia) and Merck (Darmstadt, Germany), respectively. Complementary single stranded DNA (ssDNA, 5′ -TTA TAT ACT TAA AAG CAA TA-3′ and 5′ -TAT TGC TTT TAA GTA TAT AA-3′), and complementary thiolated oligonucleotides (HS-ssDNA) having the same nucleotide sequence as ssDNA but with $HS-(CH_2)_6-$ termination at the 5′ ends were supplied by Proligo. The disulfide bonds in the thiol-modified oligonucleotides were cleaved by standard DTT (dithiothreitol) treatment before use. All chemicals were used as received. Water was purified by a Milli-Q water purification system. All glassware and Teflon-coated magnetic stir bars were cleaned in aqua regia, followed by copious washing with distilled water before drying in an oven. A JEOL JEM2010 transmission electron microscope (TEM) operating at 200 kV was used to size the particles. For TEM measurements a drop of the nanoparticle solution was dispensed onto a 3 mm copper grid covered with a continuous carbon film. Excess solution was removed by an adsorbent paper and the sample was vacuum dried at room temperature. UV-visible spectroscopy of the Au nanoparticle solution was carried out on a Shimadzu UV-2450 spectrophotometer. XPS analysis of ssDNA adsorption on Au nanoparticles was carried out on a VG ESCALAB MKII spectrometer. Sample preparation for XPS analysis began with the collection of Au particles from a ssDNA–Au hydrosol mixture by centrifugation at 16,000 rpm for 45 min. The sample was then washed with distilled water and 0.3 M PBS buffer in sequence to remove the unbound ssDNA, and dried in vacuum at room temperature.

Melting point analysis of the DNA in all samples was performed on a Shimadzu UV-2450 spectrophotometer equipped with a Shimadzu DC Pico Ace 25 Peltier temperature controller. Absorbance was recorded at 1 °C intervals using a holding time of 1 min at each temperature. Other experimental parameters may be found in the respective figure captions.

2.2. Preparation of Au nanoparticles

Approximately 17 nm Au nanoparticles were prepared by the citrate reduction of $HAuCl_4$ [24,25]. An aqueous solution of $HAuCl_4$ (1 mM, 20 mL) was refluxed at 110 °C with stirring in an oil bath. 2 mL of 38.8 mM aqueous tri-sodium citrate solution was added quickly, which resulted in a series of color changes before finally arriving at a wine red solution. The mixture was refluxed for another 15 min and allowed to cool to room temperature. The smaller 5 nm citrate-protected Au nanoparticles were prepared by a different process. Briefly, 10 mL of 1 mM aqueous solution of $HAuCl_4$ was mixed with 0.8 mL of 38.8 mM aqueous sodium citrate solution used as stabilizer. 0.3 mL of 100 mM aqueous solution of $NaBH_4$ was then added dropwise under vigorous stirring, giving rise to a red Au hydrosol. The Au hydrosol was only used after ageing for 24 h to decompose the residual $NaBH_4$.

2.3. Preparation of ssDNA-stabilized Au nanoparticles

ssDNA-stabilized Au nanoparticles (5 and 17 nm) were prepared by adding 25 μL of 20 μM ssDNA solution to 200 μL of 5 nm Au nanoparticle hydrosol (~260 nM of nanoparticles) or to 200 μL of 17 nm Au particle solution (~14 nM of nanoparticles). The mixture was then aged for more than 3 h. The effect of the mole ratio of ssDNA to Au particles on the stability of ssDNA stabilized Au nanoparticles was studied by varying the amount of ssDNA solution used.

2.4. DNA hybridization involving 5 nm Au nanoparticles

DNA hybridization in the presence of small Au nanoparticles was investigated in three sets of experiments. In the first set, to three 200 μL of 5 nm Au hydrosol, 0.5, 1.3 and 2.6 nmol of ssDNA were added to stabilize the small Au nanoparticles. The mole ratio of ssDNA to Au nanoparticles was about 10 : 1, 25 : 1 and 50 : 1, respectively. Three other ssDNA–Au conjugates were similarly prepared using the same Au hydrosol and 0.5, 1.3 and 2.6 nmol of ssDNA with the complementary sequence. The ssDNA–Au conjugates were individually aged overnight. Each of the ssDNA–Au conjugates was then suspended in 0.3 M PBS buffer (0.3 M NaCl and 0.01 M phosphate) and then mixed with the complementary ssDNA–Au conjugates. DNA melting analysis was carried out on the mixture after dilution with 0.3 M PBS buffer to a final ssDNA concentration of 1 μM. In the second set of experiments, ssDNA with complementary sequences were first hybridized in 0.3 M PBS Buffer. The concentration of the hybridized DNA was fixed at 20 μM. Then to four 10 μL of the hybridized DNA solution, 190, 160, 140 and 90 μL of 0.3 M PBS buffer was introduced, followed by the addition of 0, 3, 5 and 10 μL of 3 M PBS buffer (3 M NaCl and 0.1 M phosphate). The diluted DNA solution were kept for 15 min at 80 °C and then 27, 45, and 90 μL of 5 nm Au hydrosol was added to each of them. The final concentration of ssDNA in the mixture so obtained was 1 μM and the ssDNA to Au nanoparticle ratios were the same as those in the first set of experiments. The solutions were cooled to room temperature before DNA melting analysis and the first sample (containing no Au nanoparticles) was used as the control. The third set of experiment was a slight modification of the second set of experiments, with the

addition of the Au hydrosols to the diluted DNA solutions carried out at room temperature.

2.5. Preparation of Ag seeds and Ag–Pt core–shell nanoparticles

9.6 nm citrate-stabilized Ag seeds were first synthesized from the $NaBH_4$ reduction of $AgNO_3$. Briefly, 20 mL of 1 mM aqueous $AgNO_3$ solution was mixed with 1.6 mL of 38.8 mM aqueous sodium citrate solution used as stabilizer. 0.4 mL of 112 mM aqueous $NaBH_4$ solution was then added dropwise under vigorous stirring, giving rise to a yellowish brown Ag hydrosol. The Ag hydrosol was aged for 24 h to decompose the residual $NaBH_4$ before it was used in subsequent steps. For the preparation of core–shell Ag–Pt nanoparticles, 10 mL of 1 mM aqueous solution of K_2PtCl_4 (Aldrich) was first refluxed for 1 h at 110 °C, and then a calculated amount of Ag nanoparticle solution (for a Ag to Pt ratio of 1:1) and 0.8 mL of 40 mM sodium citrate solution were added. The mixture was refluxed for 60 min to completely reduce Pt(II) to Pt(0). The Ag–Pt hydrosol so prepared was reddish brown in color and TEM examination showed an average particle size of 14.6 nm and a relatively narrow size distribution.

2.6. DNA hybridization induced assembly of Ag–Pt core–shell nanoparticles

For the preparation of thiolated ssDNA-functionalized Pt nanoparticles with the Ag cores, 1 nmol of thiol-modified ssDNA (sequence: 5′ -HS-TTA TAT ACT TAA AAG CAA TA-3′ , Proligo) and 1 nmol of thiol-modified ssDNA with the complementary sequence (5′ -HS-TAT TGC TTT TAA GTA TAT AA-3′ , Proligo) were added to two 400 μL citrate-stabilized $Ag_{core}Pt_{shell}$ hydrosols, respectively. The mole ratio of ssDNA to core–shell Ag–Pt nanoparticles was about 120:1. The hydrosols were then aged for 10 h and a further 6 h in 0.2 M PBS buffer (0.2 M NaCl and 0.01 M phosphate). Finally 200 μL of each mixture was suspended in 0.3 M PBS buffer (0.3 M NaCl and 0.01 M phosphate) and mixed together. Color bleaching from reddish brown occurred within two to three hours and a precipitate was formed in ten hours, indicating that the core-augmented Pt nanoparticles had been successfully assembled by DNA hybridization.

3. Results and discussion

3.1. Stabilization of small Au nanoparticles by ssDNA

In the absence of ssDNA, the Au nanoparticle solutions (5 and 17 nm) were unstable in 0.1 M NaCl solution. Color change from red to blue would occur immediately upon contacting the Au nanoparticle solution with 0.1 M PBS buffer because of the aggregation of nanoparticles in the solution. However, for a mixture of 5 nm Au nanoparticle solution and ssDNA solution which had been aged for 3 h, the addition of PBS buffer (up to 0.6 M) did not bring about any color change (particle aggregation), suggesting the stabilization of the Au nanoparticles by ssDNA. The ssDNA stabilized Au nanoparticles were stable in NaCl solutions up to a maximum tested concentration of 0.6M.

Fig. 1 shows the UV-visible spectra of ssDNA stabilized 5 nm Au nanoparticles after 16 h of ageing in different PBS buffers. Changes in the position and the intensity of the Au surface plasmon resonance band (SPR, indication of particle agglomeration) were measurable only when the concentration of the PBS buffer had increased to 0.6 M, as shown by the red-shift from 523 to 534 nm. Increasing the solution temperature up to 110 °C also did not destabilize the ssDNA capped 5 nm Au nanoparticles.

The adsorption of ssDNA on Au nanoparticles was assayed by XPS. The presence of a N 1s peak in the XPS spectrum is indication of ssDNA adsorption since pristine gold nanoparticles exposed to only the PBS buffer (without ssDNA) yielded no nitrogen signal. As the N 1s signal must originate exclusively from the nitrogen-bases in ssDNA, the relative strengths of adsorption on Au nanoparticles of different sizes could be estimated from a comparison of the N 1s integrated peak areas. From the N 1s spectra of ssDNA adsorption on 5 and 17 nm Au nanoparticles shown in Fig. 2, the more intense N 1s peak in the former identifies positively a stronger adsorption of ssDNA on smaller Au nanoparticles. XPS measurements also showed that the adsorbed ssDNA was not removable by repeated rinsing with water or PBS buffer, or by heating the ssDNA–Au nanoparticle conjugates to 110 °C.

It is reasonable that the Au nanoparticles interacted with ssDNA by coordinating with the nitrogen bases in the nucleotides. Interaction of this nature has been suggested by Herne et al. [26] for gold films and by Storhoff et al. [27] for 16 nm Au nanoparticles. However, interaction as strong as that between 5 nm Au nanoparticles and ssDNA was not expected, and its strong dependence on particle size has not been reported. Sandström et al. [28] expected such nonspecific

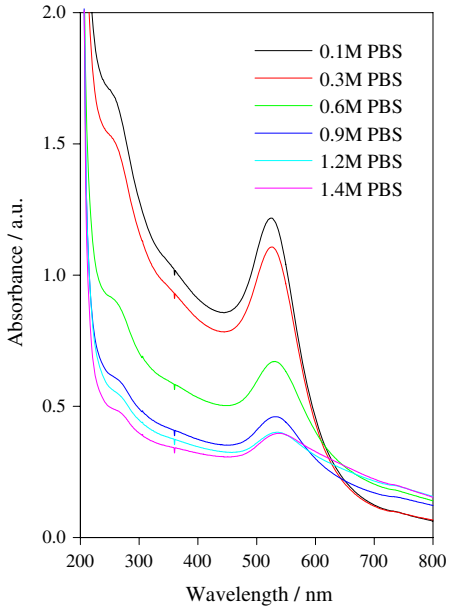

Fig. 1. UV-visible spectra of ssDNA stabilized Au nanoparticle in different PBS buffers for 16 h.

interaction to be reduced by the high curvature of small particles, and cited the experimental results of Zanchet et al. [29] as supporting evidence. However, a closer look at Alivasatos' experiments revealed that the 5 nm Au nanoparticles had been passivated by K_2BSPP (dipotassium bis(p-sulfonatophenyl)phenylphosphane dehydrate) prior to oligonucleotide functionalization, hence the reduction in nonspecific binding could have been the effort of the surface passivation procedure and not by any intrinsic particle size effect. Another significant observation in the current work is the lack of apparent correlation between the strength of interaction and the nucleotide sequence in ssDNA. This observation differs from the results of Storhoff et al. [27], who found the stability of DNA stabilized 16 nm gold nanoparticles to be dependent on the DNA base sequence. In order to verify that there is a *strong and undifferentiated affinity between the nitrogen bases and the surface atoms of small Au nanoparticles,* we have repeated the experiments with sequences such as 5′ -ATG GCA ACT ATA CGC GCT AG-3′ , 5′ -AAA CGA CTC TAG CGC GTA TA-3′ , 5′ -TAT TGC TTT TAA GTA TAT AA-3′ , 5′ -AAA AAA AAA AAA AAA AAA AA-3′ and 5′ -TTT TTT TTT TTT TTT TTT TT-3′ . In all cases the stability of the ssDNA-5 nm Au nanoparticle conjugates was similar to the results shown in Figs. 1 and 2.

Varying the mole ratio of ssDNA to 5 nm Au particles from 10 to 150 had negligible effect on the stability of the ssDNA-capped Au nanoparticles. This is taken to imply that the adsorption of ssDNA on the surface of the 5 nm Au nanoparticles reaches saturation relatively easily. We have also examined the stability of ssDNA stabilized 17 nm Au nanoparticles. In the range of molar ratio of ssDNA to 17 nm Au nanoparticles from 170 to 2600, the stability of ssDNA stabilized 17 nm Au particles was rather weak, and color change from red to purple to blue was imminent several

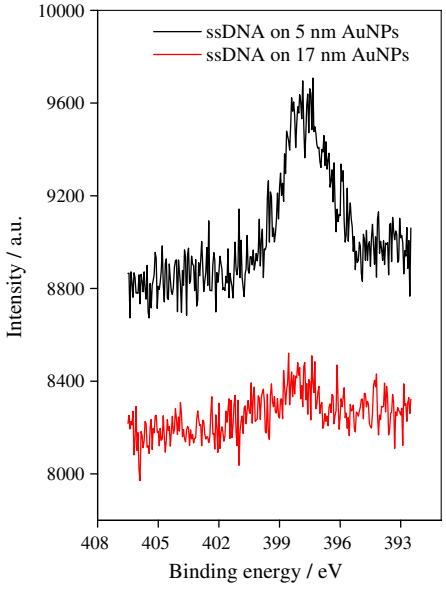

Fig. 2. N 1s XPS spectra of ssDNA on 5 (black line) and 17 nm (red line) Au nanoparticles. (For interpretation of the references to colour in this figure legend, the reader is referred to the web version of this article.)

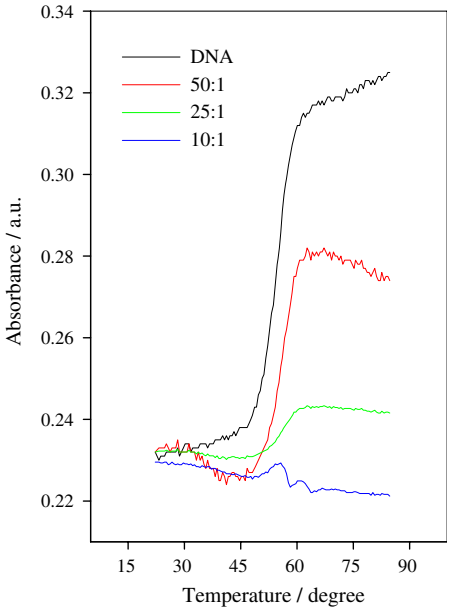

Fig. 3. "Melting analysis" of the oligonucleotide–Au conjugates formed in the first set of experiments. Absorbance was recorded at 260 nm with an oligonucleotide concentration of 1 μM in the solution.

minutes after the addition of 0.1 M PBS solution. The observation therefore corroborated the XPS measurements in Fig. 2 (red line).

3.2. Inhibition of DNA hybridization by small Au nanoparticles

The presence of strong nonspecific interaction between ssDNA and small Au nanoparticles was also convincingly

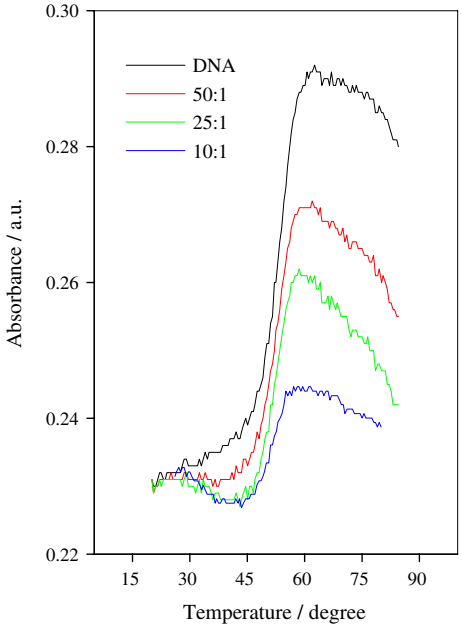

Fig. 4. "Melting analysis" of matching oligonuceotides in the presence of small Au nanoparticles (second set of experiment). Different amount of small Au nanoparticles were added to the de-hybridized DNA solution at 80 °C and then the solution was cooled down to room temperature before the melting point measurement. Absorbance was recorded at 260 nm with an oligonucleotide concentration of 1 μM in the solution.

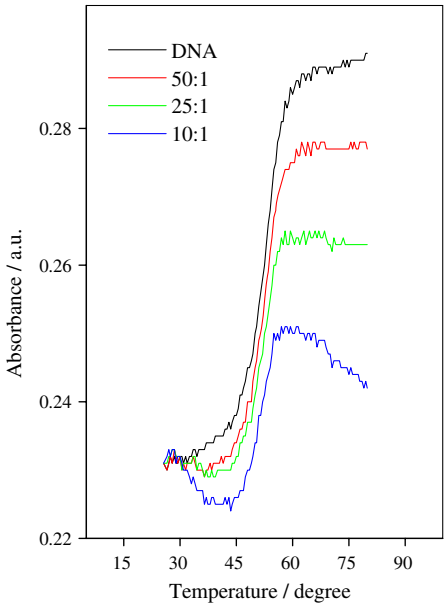

Fig. 5. "Melting analysis" of the four DNA–Au systems formed in the third set of experiment. Different amount of small Au nanoparticles were added to the hybridized DNA solution in 0.3 M PBS buffer at room temperature. Absorbance was recorded at 260 nm with an oligonucleotide concentration of 1 μM in the solution.

demonstrated by the inhibition of DNA hybridization in the presence of small Au nanoparticles. The evidence came from the measurements of DNA melting points of three sets of ssDNA-Au conjugates described in the Materials and Methods Section. Fig. 3 shows the melting analysis of "hybridized" ssDNA–Au conjugates formed in the first set of experiments. ssDNA solution of the same concentration and sequence hybridized in the absence of the small Au nanoparticles was used as the control. For the convenience of comparison, the melting curves in this Figure (and also those in (Figs. 4, 5 and 9)) have been vertically shifted so that all melting curves share the same starting baseline. Since the Au nanoparticles were not aggregated under the experimental conditions, there were no changes in the SPR signal of the Au particles that might interfere with the measurements at 260 nm. The inhibition of DNA hybridization is shown by the broadening, or the lack of a melting transition. Fig. 3 shows clearly that the extent of inhibition increased with decreasing DNA to Au nanoparticle ratio. In particular DNA hybridization was almost completely suppressed at the 10 : 1 ratio. Some hybridized ssDNA did exist at high DNA to Au nanoparticle ratios because of the presence of free ssDNA in these systems. The data also show that Au nanoparticles were completely saturated with ssDNA at ssDNA/Au nanoparticle ratios of about 25. It may therefore be inferred that the non-specific interaction between ssDNA and small Au nanoparticles, which prevented the ssDNA from aligning optimally for hybridization, was the cause for inhibition of DNA hybridization.

The second set of experiments was used to evaluate the preference of ssDNA in choosing between DNA hybridization and the stabilization of small Au nanoparticles. In these experiments hybridized ssDNA was first de-hybridized by keeping the solution at 80 °C for 15 min (the melting point of DNA used in this work is ca. 53.8 °C according to Fig. 3). The most remarkable observation is the lack of particle aggregation when the small Au nanoparticles were introduced in the presence of 0.3 M PBS buffer, a strong electrolyte which would readily salt out the Au nanoparticles (color change from red to blue) in the absence of ssDNA. This shows that the enhanced

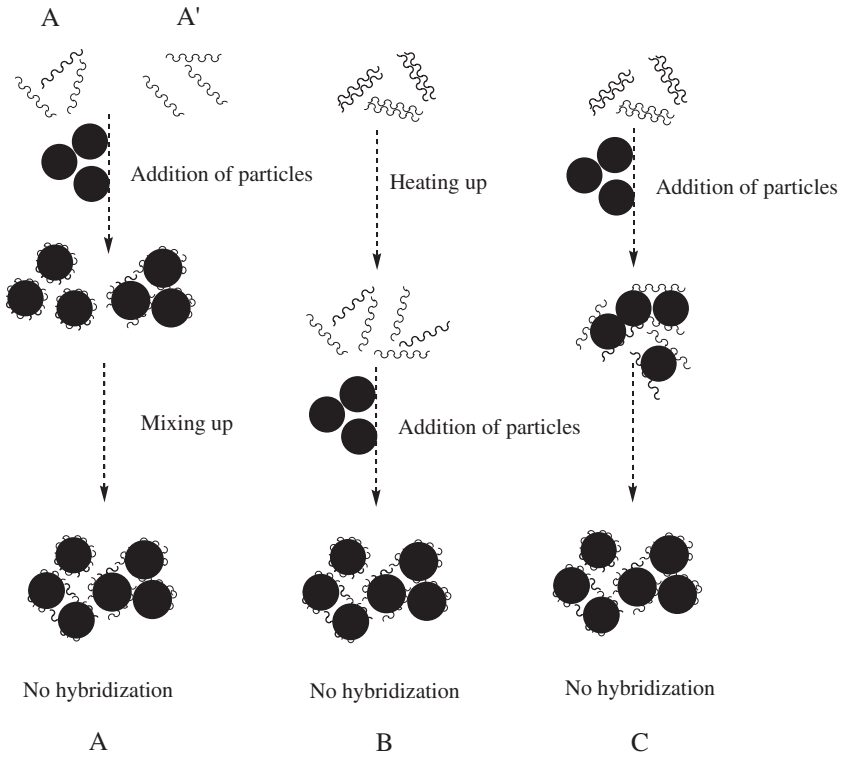

Scheme 1. Models of inhibition of DNA hybridization by small Au nanoparticles.

stability of Au nanoparticles in PBS buffer was imparted by ssDNA and not by thermal redispersion. It also indicates that the ssDNA stabilization of small Au nanoparticles is kinetically facile. From the melting curves of four hybridized DNA solutions shown in Fig. 4, the inhibition of DNA re-hybridization by small Au nanoparticles is clearly evident, suggesting that the oligonucleotide stabilization of small Au nanoparticles is preferable to forming double helices between complementary DNA sequences.

Sandström et al. [28] reported that unmodified double-stranded DNA could bind nonspecifically to the surface of the negatively charged 13 nm Au nanoparticles. They hypothesized the possibility of strand separation involving a short section of double stranded DNA that allowed the Au particles to bind to the exposed nitrogen bases. However, they did not provide direct experimental evidence in support of their hypothesis. We too have observed the de-stabilization of hybridized DNA by small Au nanoparticles. In the third set of experiments using a low DNA to Au nanoparticle ratio (10 : 1), some light color transition from red to light purple (due to a limited extent of particle aggregation) was observed when small Au nanoparticles were added to the hybridized DNA solution in 0.3 M PBS buffer. However, the DNA–Au system was subsequently quite stable; and no further changes occurred even after several weeks of storage. On the other hand, no color change was detected when the DNA to Au nanoparticle ratio was sufficiently high (25 : 1 and 50 : 1) to fully suppress the nanoparticle aggregation. We again analyzed the melting temperature (T_m) of the DNA–Au systems formed in the third set of experiments. The melting curves in Fig. 5 are similar to those in Fig. 4, showing the inhibition of DNA hybridization by small Au nanoparticles. This inhibition shows that the interaction between the oligonucleotide backbone and small nanoparticle surface was strong enough to disrupt the hydrogen bonds formed between complementary oligonucleotides and thus hybridized DNA was separated into single strands for the stabilization of small Au nanoparticles.

The inhibition of DNA hybridization by small Au nanoparticles in the three sets of experiments could be understood by the models shown in Scheme 1. The models interpret satisfactorily the inhibition of DNA hybridization by small Au nanoparticle, and the stabilization of small Au nanoparticles by ssDNA. The proposed structures in Scheme 1 are more than hypothetical as they suggest the formation of geometrically distinct features that can be identified by analytical TEM. The TEM images of ssDNA stabilized 5 nm Au nanoparticles in Fig. 6 validate the expectation. As a control, the TEM image of citrate stabilized 5 nm Au nanoparticles without ssDNA was also taken (Fig. 7). The lack of extensive particle binding in the latter is fairly obvious by comparison.

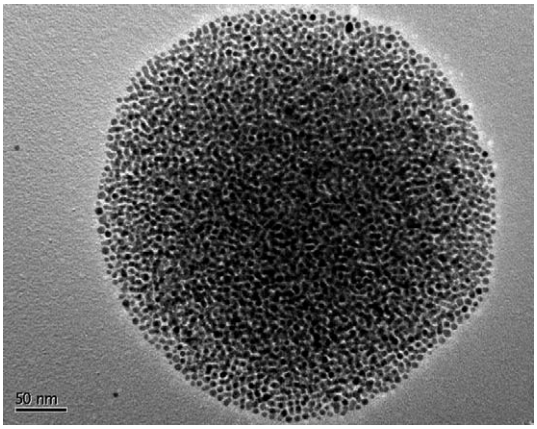

Fig. 6. TEM images of 5 nm normal oligonucleotide-stabilized Au nanoparticles.

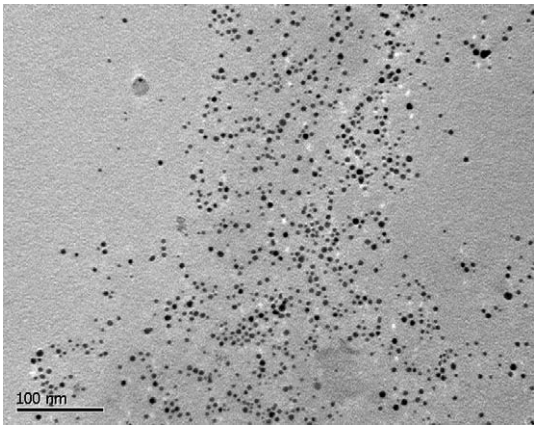

Fig. 7. TEM image of citrate stabilized 5 nm Au nanoparticles (no ssDNA).

The UV-visible spectra of citrate-stabilized 5 nm Au nanoparticles and ssDNA-stabilized 5 nm Au nanoparticles (with ssDNA to Au particle ratio of 10 : 1) in aqueous solutions are shown in Fig. 8. There was a modest red-shift in the surface plasmon resonance band from 517 to 523 nm after the ssDNA stabilization of the gold nanoparticles, which is yet another evidence for the existence of aggregated structures in the

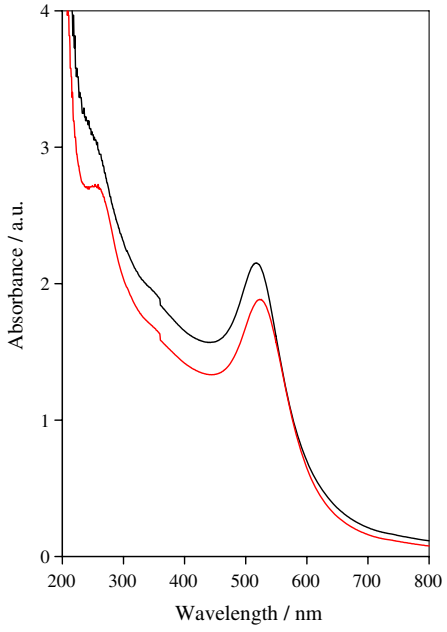

Fig. 8. Comparison of UV-visible spectral features between citrate stabilized (black line) and ssDNA stabilized 5 nm Au nanoparticles (red line) in aqueous solutions. (For interpretation of the references to colour in this figure legend, the reader is referred to the web version of this article.)

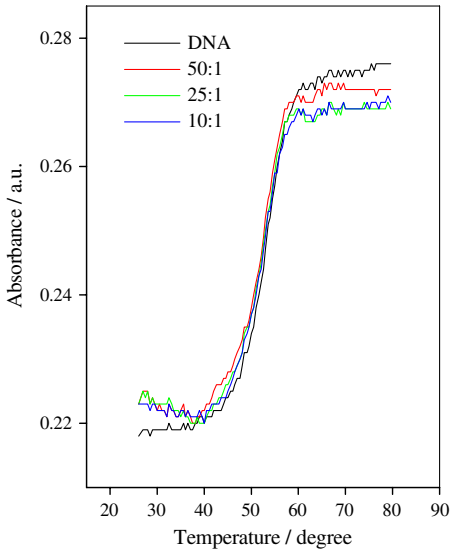

Fig. 9. "Melting analysis" of complementary oligonuceotides in the presence of 17 nm Au nanoparticles.

solution.The inhibition of DNA hybridization by metal nanoparticles and the stability of ssDNA-stabilized metal nanoparticles in NaCl solutions are not unique to small Au nanoparticles only. Similar results were obtained when we repeated the experiments with small (3.6 nm) Pt nanoparticles. As most of the reported successes in DNA hybridized induced assembly of Au nanoparitcles have been based on relatively large particles [4,8,16,18,23], the nonspecific interaction is probably weaker between oligonucleotides and large Au nanoparticles. The inference was experimentally confirmed as follows: We repeated the inhibition experiments (all three sets) using 17 nm Au nanoparticles. Aggregation of the nanoparticles (as shown by color change from red to blue) occurred instantaneously in the hybridization solution and precipitates were formed within 30 min. The melting transition of hybridized DNA was unchanged in the presence of 17 nm Au nanoparticles (Fig. 9), showing that these larger Au nanoparticles did not inhibit DNA hybridization. This is in strong contrast to the case of 5 nm Au particles where neither color change nor precipitation occurred. The lack of stability of 17 nm Au nanoparticles in NaCl solutions even with the ssDNA presence confirms the weaker nonspecific interaction between ssDNA and large Au nanoparticles.

The nonspecific interaction between the oligonucleotide backbone and metal nanoparticles responsible for the stability of the latter in salt solutions could interfere with DNA hybridization by preventing ssDNA from aligning optimally for hybridization (the ssDNA wraps around the metal nanoparticles instead of being fully stretched out and perpendicular to the nanoparticle surface). The results here also satisfactorily rationalized the failure of Mirkin's protocol in assembling small metal nanoparticle systems. Hence any attempt to assemble small metal nanoparticles by DNA hybridization requires some control of the nonspecific interaction. Two possible solutions may be put forward: The first method uses appropriate surface treatments to screen the nonspecific interaction. Unfortunately, the success of this method with small Au nanoparticles (using K_2BSPP) [29,30] and Au films (using competitive 6-mercapto-1-hexanol adsorption) [21] could not be extended to other nanoparticles such as Pt. The second and more general solution is to increase the particle size to weaken the nonspecific interaction. However, most current methods of preparation of single metal nanoparticles in aqueous environment are unable to produce particles of arbitrary sizes [31,32]. In the following sections we will demonstrate a core–shell assisted Pt particle assembly induced by DNA hybridization where the diameters of the Pt nanoparticles have been increased through a core–shell construction by successive reduction (also known as seed-mediated growth) seeded by the nanoparticles of an appropriate core metal (9.6 nm Ag nanoparticles).

3.3. Assembly of core–shell Ag–Pt nanoparticles by DNA hybridization

The surface modification of $Ag_{core}Pt_{shell}$ nanoparticles by complementary thiol-modified oligonucleotides and the ensuing DNA hybridization induced assembly of these particles have been described in detail in the Materials and Methods Section. The difference between this work and the work of Cao et al. [15] in 2001 should perhaps be emphasized: core–shell assisted assembly of $Ag_{core}Au_{shell}$ core–shell particles was used by Mirkin to address the lack of affinity between the oligonucleotides and the Ag surface, whereas the core–shell geometry was used in this study to artificially enlarge the Pt particles so as to reduce the extent of nonspecific interaction inhibiting the hybridization-induced assembly.

Similar to the 5 nm Au nanoparticles shown earlier, the small Pt nanoparticles (3.6 nm) capped by unmodified ssDNA were stable in salt solutions up to 0.6 M NaCl at room temperature. On the other hand, the core-enlarged Pt nanoparticles, with or without ssDNA presence, were unstable in salt solutions and particle aggregation occurred readily in 0.2 M PBS buffer. This is clear evidence of the reduced level of stabilization by nonspecific interaction in the enlarged particles.

Fig. 10 shows the TEM images of the $Ag_{core}Pt_{shell}$ nanoparticles prepared in this study. Pt deposition increased

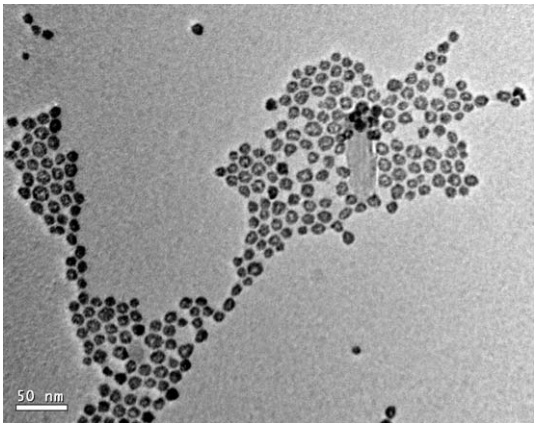

Fig. 10. TEM image of bimetallic core–shell Ag–Pt nanoparticles prepared by the seed mediated growth process using citrate-stabilized Ag seeds.

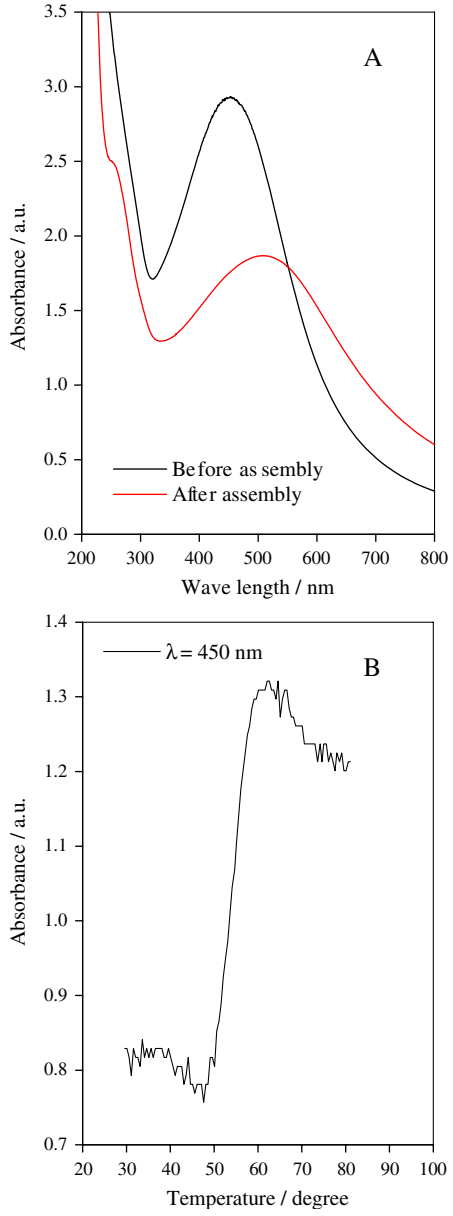

Fig. 11. (A) UV-Visible spectra of core–shell Ag–Pt nanoparticles before (black line) and after (red line) DNA hybridization induced assembly. (B) "Melting analysis" of core–shell Ag–Pt nanoparticles assembled by DNA hybridizations. Absorbance was recorded at 450 nm with a DNA concentration of 1 μM in the solution on a Shimadzu UV-2450 spectrophotometer equipped with a Shimadzu DC Pico Ace 25 Peltier temperature controller. The absorbance was recorded at 1 °C intervals using a hold time of 1 min at each temperature. (For interpretation of the references to colour in this figure legend, the reader is referred to the web version of this article.)

the size of the Ag seeds from 9.6 to 14.6 nm. The core–shell structure was confirmed by a phase transfer method described elsewhere [33]. The most interesting property of the bimetallic core–shell particles is the retention of the optical properties of the Ag cores [33], which allows the particles to be characterized by the Ag surface plasmon resonance (SPR) band; and the DNA hybridization induced aggregation of the nanoparticles by the red-shifting of the SPR band.

The UV-visible spectra of DNA hybridization induced assembly of Pt nanoparticles with the Ag cores are shown in Fig. 11A. Successful assembly can be inferred from the broadening and the red shifting of the Ag SPR band from 450 to 510 nm. In addition, the "melting curve" of the aggregates obtained by monitoring the spectral changes at 450 nm is shown in Fig. 11B. When a colloidal solution containing the assembled $Ag_{core}Pt_{shell}$ nanoparticles was heated above the "melting temperature" (T_m) of the hybridized oligonucleotides, the reddish brown color of the solution and the surface plasmon band of isolated $Ag_{core}Pt_{shell}$ particles at 450 nm, characteristic of disassembled $Ag_{core}Pt_{shell}$ nanoparticles, would appear again. This "melting transition" from the bound state to the totally de-hybridized state was extremely sharp, which is common among DNA-metal bioconjugates [4,8,16,18].

TEM images (Fig. 12A) of the assembled system indeed show large aggregates of the core–shell Ag–Pt nanoparticles forming three-dimensional organized structures on the TEM grid. A control experiment was carried out in which 200 μL of thiol-modified ssDNA stabilized $Ag_{core}Pt_{shell}$ hydrosol was mixed with the same bimetallic hydrosol functionalized by oligonucleotides with mismatched base sequences and different lengths (5′ -HS-CGC ATT CAG GAT-3′) in 0.3 M PBS buffer. No apparent changes in the UV-visible spectral features or the formation of regular assembly detectable by TEM were found (Fig. 12B). TEM only showed randomly dispersed particles for this case since DNA induced assembly was disabled by the lack of matching nucleotide sequences.

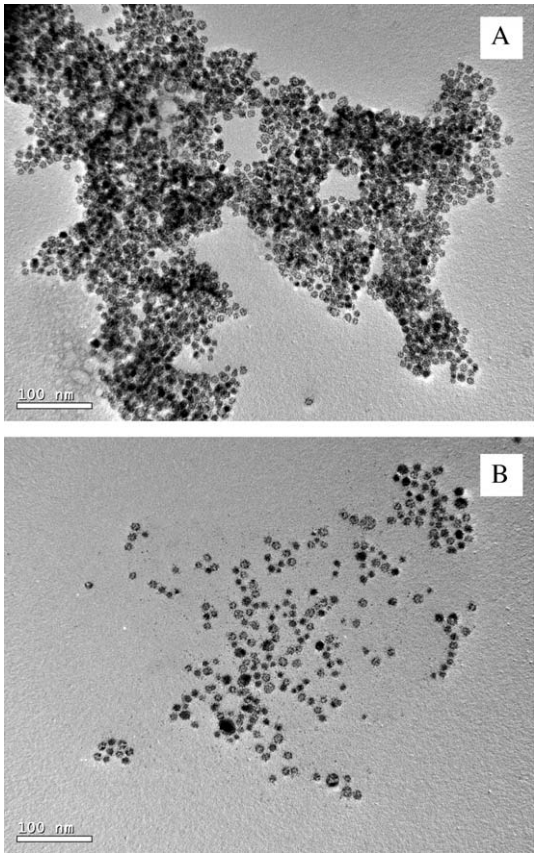

Fig. 12. (A) TEM image of the core–shell Ag–Pt nanoparticles assembled by DNA hybridization. (B) TEM image of the mixture of core–shell Ag–Pt nanoparticles functionalized by non-complementary thiolated oligonucleotides.

4. Conclusions

This article shows convincingly the presence of strong nonspecific interaction between the backbone of oligonucleotides and the surface of small metal nanoparticles, which stabilizes the nanoparticles in high salt solutions, but is otherwise prohibitive of the hybridization of matching DNA sequences. DNA melting analysis showed that the non-specific adsorption was kinetically facile and is strong enough to disrupt the hydrogen bonds between complementary nucleotide sequences established previously. This study also reveals that the nonspecific interaction could be weakened by increasing the particle size. Thus a core–shell assisted method was developed to enable the assembly of Pt nanoparticles by DNA hybridization. The key feature of this method is the use of core–shell construction to artificially increase the apparent Pt particle size to reduce the nonspecific interaction between single stranded DNA and the metal nanoparticle surface. Non–specific interaction is prevalent in many metal nanoparticles, such as Au, Ag, Pt and Cu, and has been the major obstacle in the DNA induced assembly of these particles [34,35]. The use of enlarged particle size to reduce the nonspecific interaction appears to be a generic method that could lead to more dissimilar metals to be assembled by DNA hybridization.

Acknowledgements

The authors would like to acknowledge the financial support from Agency for Science, Technology and Research (project number 022-101-0038). JY would like to acknowledge the National University of Singapore for his research scholarship.

References

[1] J.J. Storhoff, C.A. Mirkin, Programmed materials synthesis with DNA, Chem. Rev. 99 (1999) 1849–1862.
[2] R.A. Reynolds III, C.A. Mirkin, R.L. Letsinger, Homogeneous, nanoparticle-based quantitative colorimetric detection of oligonucleotides, J. Am. Chem. Soc. 122 (2000) 3795–3796.
[3] J.L. Coffer, S.R. Bigham, R.F. Pinizzotto, H. Yang, Characterization of quantum-confined CdS nanocrystallites stabilized by deoxyribonucleic acid (DNA), Nanotechnology 3 (1992) 69–76.
[4] C.A. Mirkin, R.L. Letsinger, R.C. Mucic, J.J. Storhoff, A DNA-based method for rationally assembling nanoparticles into macroscopic materials, Nature 382 (1996) 607–609.
[5] A.P. Alivisatos, K.P. Johnsson, X. Peng, T.E. Wilson, C.J. Loweth, M.P. Bruchez Jr., P.G. Schultz, Organization of 'nanocrystal molecules' using DNA, Nature 382 (1996) 609–611.
[6] J.L. Coffer, S.R. Bigham, X. Li, R.F. Pinizzotto, Y.G. Rho, R.M. Pirtle, I.L. Pirtle, Dictation of the shape of mesoscale semiconductor nanoparticle assemblies by plasmid DNA, Appl. Phys. Lett. 69 (1996) 3851–3853.
[7] R. Elghanian, J.J. Storhoff, R.C. Mucic, R.L. Letsinger, C.A. Mirkin, Selective colorimetric detection of polynucleotides based on the distance-dependent optical properties of gold nanoparticles, Science 277 (1997) 1078–1080.
[8] R.C. Mucic, J.J. Storhoff, C.A. Mirkin, R.L. Letsinger, DNA-directed synthesis of binary nanoparticle network materials, J. Am. Chem. Soc. 120 (1998) 12674–12675.
[9] E. Braun, Y. Eichen, G. Ben-Yoseph, DNA-templated assembly and electrode attachment of a conducting silver wire, Nature 391 (1998) 775–778.
[10] M. Cassell, W.A. Scrivens, J.M. Tour, Assembly of DNA/fullerene hybrid materials, Angew. Chem. Int. Ed. 37 (1998) 1528–1531.
[11] C.M. Niemeyer, W. Burger, J. Peplies, Covalent DNA-streptavidin conjugates as building blocks for novel biometallic nanostructures, Angew. Chem. Int. Ed. 37 (1998) 2265–2268.
[12] T.A. Taton, R.C. Mucic, C.A. Mirkin, R.L. Letsinger, The DNA-mediated formation of supramolecular mono-and multilayered nanoparticle structures, J. Am. Chem. Soc. 122 (2000) 6305–6306.
[13] G.P. Mitchell, C.A. Mirkin, R.L. Letsinger, Programmed assembly of DNA functionalized quantum dots, J. Am. Chem. Soc. 121 (1999) 8122–8123.
[14] Z. Li, R. Jin, C.A. Mirkin, R.L. Letsinger, Multiple thiol-anchor capped DNA-gold nanoparticle conjugates, Nucleic Acid Res. 30 (2002) 1558–1562.
[15] Y. Cao, R. Jin, C.A. Mirkin, DNA-modified core-shell Ag/Au nanoparticles, J. Am. Chem. Soc. 123 (2001) 7961–7962.
[16] J.J. Storhoff, A.A. Lazarides, R.C. Mucic, C.A. Mirkin, R.L. Letsinger, G.C. Schatz, What controls the optical properties of DNA-linked gold nanoparticle assemblies? J. Am. Chem. Soc. 122 (2000) 4640–4650.
[17] S.J. Park, A.A. Lazarides, C.A. Mirkin, P.W. Brazis, C.R. Kannewurf, R.L. Letsinger, The electrical properties of gold nanoparticle assemblies linked by DNA, Angew. Chem. Int. Ed. 39 (2000) 3845–3848.
[18] J.J. Storhoff, R. Elghanian, R.C. Mucic, C.A. Mirkin, R.L. Letsinger, One-pot colorimetric differentiation of polynucleotides with single base imperfections using gold nanoparticle probes, J. Am. Chem. Soc. 120 (1998) 1959–1964.
[19] T.A. Taton, C.A. Mirkin, R.L. Letsinger, Scanometric DNA array detection with nanoparticle probes, Science 289 (2000) 1757–1760.
[20] S.J. Park, T.A. Taton, C.A. Mirkin, Array-based electrical detection of DNA with nanoparticle probes, Science 295 (2002) 1503–1506.
[21] M.L. Sauthier, R.L. Carroll, C.B. Gorman, S. Franzen, Nanoparticle layers assembled through DNA hybridization: characterization and optimization, Langmuir 18 (2002) 1825–1830.
[22] Y. Maeda, H. Tabata, T. Kawai, Two-dimensional assembly of gold nanoparticles with a DNA network template, Appl. Phys. Lett. 79 (2001) 1181–1183.
[23] R. Jin, G. Wu, Z. Li, C.A. Mirkin, G.C. Schatz, What controls the melting properties of DNA-linked gold nanoparticle assemblies? J. Am. Chem. Soc. 125 (2003) 1643–1654.
[24] K.C. Grabar, R.G. Freeman, M.B. Hommer, M.J. Natan, Preparation and characterization of Au colloid monolayers, Anal. Chem. 67 (1995) 735–743.
[25] L.A. Gearheart, H.J. Ploehn, C.J. Murphy, Oligonucleotide adsorption to gold nanoparticles: a surface-enhanced Raman spectroscopy study of intrinsically bent DNA, J. Phys. Chem., B 105 (2001) 12609–12615.
[26] T.M. Herne, M.J. Tarlov, Characterization of DNA probes immobilized on gold surfaces, J. Am. Chem. Soc. 119 (1997) 8916–8920.
[27] J.J. Storhoff, R. Elghanian, C.A. Mirkin, R.L. Letsinger, Sequence-dependent stability of DNA-modified gold nanoparticles, Langmuir 18 (2002) 6666–6670.
[28] P. Sandström, M. Boncheva, B. Åkerman, Nonspecific and thiol-specific binding of DNA to gold nanoparticles, Langmuir 19 (2003) 7537–7543.
[29] D. Zanchet, C.M. Nicheel, W.J. Parak, D. Gerion, A.P. Alivisatos, Electrophoretic isolation of discrete Au nanocrystal/DNA conjugates, Nano Lett. 1 (2001) 32–35.
[30] C.J. Loweth, W.B. Caldwell, X. Peng, A.P. Alivisatos, P.G. Schultz, DNA-based assembly of gold nanocrystals, Angew. Chem. Int. Ed. 38 (1999) 1808–1812.
[31] J. Yang, J.Y. Lee, T.C. Deivaraj, H.P. Too, An improved procedure for preparing smaller and nearly monodispersed thiol-stabilized platinum nanoparticles, Langmuir 19 (2003) 10361–10365.
[32] J. Yang, J.Y. Lee, T.C. Deivaraj, H.P. Too, A highly efficient phase transfer method for preparing alkylamine-stabilized Ru, Pt, and Au nanoparticles, J. Colloid Interface Sci. 277 (2004) 95–99.
[33] J. Yang, J.Y. Lee, L.X. Chen, H.P. Too, A phase-transfer identification of core–shell structures in Ag–Pt nanoparticles, J. Phys. Chem. B 109 (2005) 5468–5472.
[34] M. Zheng, F. Davidson, X. Huang, Ethylene glycol monolayer protected nanoparticles for eliminating nonspecific binding with biological molecules, J. Am. Chem. Soc. 125 (2003) 7790–7791.
[35] M.A. Hayat, in: Colloid Gold: Principles, Methods, and Applications, vol. 1, Academic Press, New York, 1989, p. 3.